Simulation Studies of Space-Charge-Dominated Beam Transport in Large Aperture Ratio Quadrupoles*

W.M. Fawley, L.J. Laslett, C.M. Celata, A. Faltens
Lawrence Berkeley Laboratory, University of California
Berkeley, CA 94720 USA
I. Haber
Naval Research Laboratory
Washington, D.C. USA

Abstract

For many cases of interest in the design of heavy-ion fusion accelerators, the maximum transportable current in a magnetic quadrupole lattice scales as $(a/L)^2$ where a is the useful dynamic aperture and L is the half-lattice period. There are many cost benefits to maximizing the usable aperture which must be balanced against unwanted effects such as possible emittance growth and particle loss from anharmonic fringe fields. We have used two independent simulation codes to model space-charge dominated beam transport both in an azimuthally-pure quadrupole FODO lattice design and in a more conventional design. Our results indicate that careful matching will be necessary to minimize emittance growth and that (a/L) ratios of 0.2 or larger are possible for particular parameters.

I. Introduction

An important issue in the design of heavy ion fusion (HIF) drivers is the dynamic aperture of short quadrupoles which immediately follow the transition from electrostatic to magnetostatic focusing. This importance stems from the maximum transportable current for a highly space-charge depressed beam scaling as the usable beam aperture, a_b, squared:

$$I_{max} \approx \left(\frac{a_b}{2L}\right)^2 I_o \, \frac{A\gamma^3\beta^3}{2Q}\,\sigma_o^2 \qquad (1)$$

Here I_o is the proton "Alfven current", 31.07 MA, σ_o is the phase advance per lattice period $2L$, A and Q are the atomic mass and charge state respectively of the ion species, and γ and β have the normal Lorentz definitions. Since a large I_{max} permits decreasing the required number of beamlets and thus more efficient use of the accelerating core cross-section, there is a great premium in making the inverse aperture ratio (a_b/L) as large as possible.

The usable beam aperture a_b may be defined as that above which the beam suffers unacceptable emittance growth and/or particle loss over transport distances of interest. Both these phenomena generally occur due to nonlinearities in the net focusing forces (*i.e.* external minus space charge). Such nonlinearities are inevitably present whenever the external focusing contains higher order multipole (*e.g.* dodecapole) moments or fringe fields (*e.g.* pseudo-octupoles [1] which arise from the second longitudinal derivative of the quadrupole moment). Although these effects are present to some degree in all strong focusing systems, FODO lattices in HIF induction accelerators are somewhat unusual in two respects: 1) Beam space-charge forces lead to very high tune depressions ($\sigma_o/\sigma \geq 10$ or more where σ is the space-charge depressed phase advance); this makes it unclear whether the usable beam aperture can be estimated from "single particle" results. 2) The high σ_o's ($\sim 72°$) true for many HIF driver designs imply relatively large AG flutter motion which may lead to poor net cancellation of fringe field and multipole forces compared to the more usual low σ_o case.

*Work supported by the Director, Office of Energy Research, Office of Fusion Energy, U.S. Dept. of Energy under Contracts No. DE-AC03-76SF00098 and DE-AI05-92ER54177.

II. Magnet Designs

A. "Conventional" Multipole Suppression

As a/L becomes large and the relative contribution of fringe fields increases, serious attention must be paid to the coil end topology. Our present work builds upon earlier designs [2] in which higher order multipoles disappear in the z-integrated sense, *i.e.*

$$\int_{-\infty}^{+\infty} dz \int_{-\pi}^{+\pi} d\theta\, A_z(r,\theta,z)\cos(4l+2)\theta = 0 \qquad (2)$$

for $l \neq 0$. Presuming time-independent coil currents, the zth component of the vector potential may be replaced by that of the current density J. In the absence of transverse motion, particles traveling through isolated magnets with this topology will suffer no net kick due to the higher order multipoles. In the real world, however, transverse motion associated with emittance and AG flutter prevents the cancellation from being absolute.

The simplest (and probably most compact) coil end topology is that of right angles with the coil turns of each individual half-period quadrant being rectangles in the developed view (ignoring the necessary turn-to-turn connections). The angular position of each wire is then determined by replacing Eq. (2) by

$$\sum_{k=1}^{n_{wire}} L_k \cos(4l+2)\theta_k = 0 \quad \text{for } l = 1, 2, \ldots \qquad (3)$$

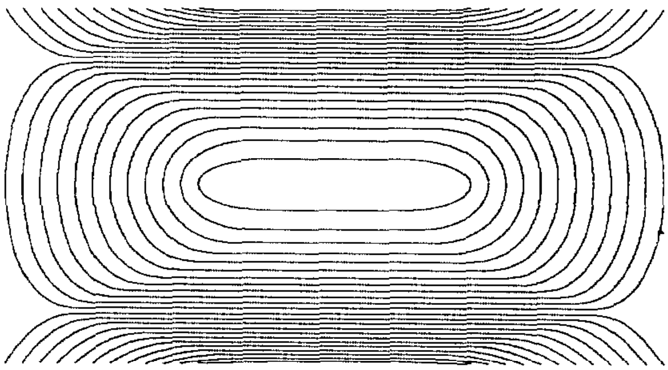

Figure 1: Top view of current windings for an ILSE prototype magnet with elliptical coil ends.

where L_k is the specified length of the k^{th} wire.

Most HIF driver designs require magnetic field magnitudes and electrical efficiencies that are possible only with superconducting cables. Present day SC cable technology requires radii of curvature ≥ 1 cm, which rules out rectangular coil ends. In addition, tight corners tend to be regions of enhanced magnetic field strength which can lead to quenching difficulties. Ref. [2] gives an analytic framework for determining a family of curves that satisfy Eq. (2). For magnetic quadrupole development associated with the Induction Linac Systems Experiment (ILSE) project, we are examining elliptical coil end curves. Fig. 1 shows a top view of the windings in one-half period; a prototype magnet with this topology is currently undergoing electrical and mechanical tests at LBL.

B. "Pure" Quadrupole Magnet Design

The multipole suppression described above is strictly relevant only to an isolated magnet. In a periodic lattice, fringe field leakage from adjacent magnets can reduce this suppression in each half-period. Moreover, AG flutter motion prevents effective suppression in the integral sense even over a full period. To overcome these limitations, one of us [LJL] suggested examining winding patterns that result in a *pure* quadrupole dependence of the fields azimuthally. The necessary surface current at radius a is

$$\vec{J}(\theta,z) = \sum_{n=1,3,5\ldots}^{\infty} \alpha_n \quad \left[\cos\left(\tfrac{n\pi z}{L}\right) \cos 2\theta \, \vec{e}_z \quad + \right.$$
$$\left. \tfrac{n\pi a}{2L} \sin\left(\tfrac{n\pi z}{L}\right) \sin 2\theta \, \vec{e}_\theta \,\right] \qquad (4)$$

and the resultant interior magnetic scalar potential is

$$\Phi_m(r,\theta,z) = \frac{\mu_0 a}{2} \sin 2\theta \sum_{n=1,3,5,\ldots}^{\infty} \alpha_n \left[\tfrac{n\pi a}{L}\right] K_2'\left(\tfrac{n\pi a}{L}\right) \times$$
$$I_2\left(\tfrac{n\pi r}{L}\right) \cos\left(\tfrac{n\pi z}{L}\right) \quad (5)$$

where I_2 and K_2 are modified Bessel functions. While the above formulas are exact only for infinite lattices, they are quite good approximations to long, periodic lattices whose wire topologies and currents change only slowly with z.

For a given choice of the longitudinal Fourier components α_n, the behavior of $K_2'(\zeta)$ for $\zeta \geq 2$ implies that the contribution of components with $n \geq 3$ near the axis become exponentially small for $a/L \geq 0.3$. In other words, as the aperture ratio a/L of a periodic lattice becomes large, the $z-$dependence of the quadrupole field components asymptotically approaches a simple sinusoid with period $2L$. Consequently, our transport studies have concentrated on the limiting case of $\alpha_n \equiv 0$ for $n \neq 1$, which we call a "one-term" magnet.

Although the magnetic fields corresponding to Eq. (5) are azimuthally pure quadrupoles, the resultant focusing has anharmonic terms due to the radial dependence of the I_2 function. To estimate the strength of these nonlinearities in a one-term magnet, we compute an average over the AG-flutter motion in one lattice period, resulting in

$$\sigma_o^2(r,\theta) = \sigma_o^2(0)\left(1 + \frac{3}{8}\left(\frac{\pi r}{L}\right)^2 - \frac{1}{8}\left(\frac{\pi r}{L}\right)^2 \cos 4\theta\right) \quad (6)$$

through terms second order in r/L. Here $\sigma_o(0)$ is the on-axis value of σ_o. One should remember that although the second and third terms on the RHS are small compared to the undepressed tune for $r \leq 0.2L$, they are relatively much larger components of the net focusing of space-charge dominated beams with $\sigma \ll \sigma_o$.

III. Simulation Code Studies

A. Code Descriptions

We employed two independently developed, electrostatic, 2D particle simulation codes for our transport studies. The first, **SHIFTXY**[3], solves fields on a uniform Cartesian $x-y$ grid and thus permits study of all azimuthal modes. The second, **HIFI**, uses an $r-\theta$ grid and presumes even symmetry about the x and y planes, thereby restricting azimuthal modes to cos $2m\theta$ dependences. Both codes include non-paraxial terms and $v_\perp \times B_z$ forces in the equation of motion and determine $\vec{B} \equiv -\nabla\Phi_m$ from Eq. (5). The initial particle loads follow either a KV or semi-Gaussian distribution in phase space (*i.e.* uniform in configuration space). The simulation "walls" are fully absorbing with radii generally $\geq$ twice the initial beam radius.

B. Emittance Growth

There are at least two related agents for emittance growth for beams transported by large aperture quadrupoles. The first arises from phase-mixed damping of macroscopic mismatch oscillations. Due to the growing relative strength of non-linearities such as the pseudo-octupole, it becomes harder and harder [*cf.* Eq.(6)] to match accurately the beam envelope parameters (x, x', y, y') as a_b/L increases. When $a_b/L \leq 0.25$, a surprisingly good match can be obtained by running an envelope code that evaluates the *total* focusing forces at the

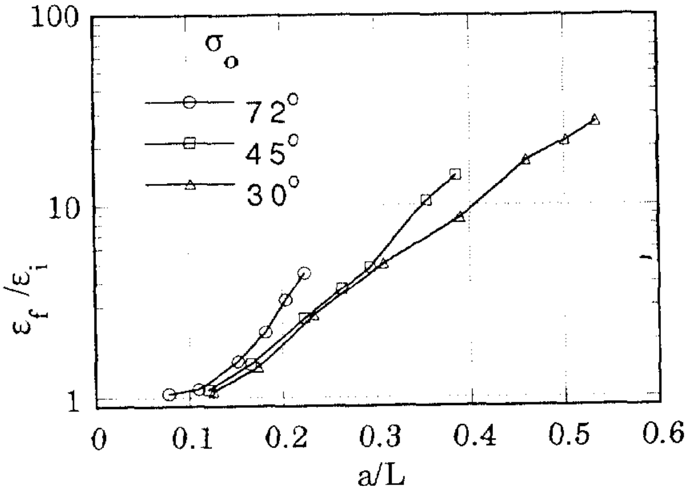

Figure 2: Relative emittance growth over 100 periods of transport in a "one-term" sinusoidal lattice versus a_b/L for three values of σ_o. Each curve was terminated when particle losses exceeded a few per cent.

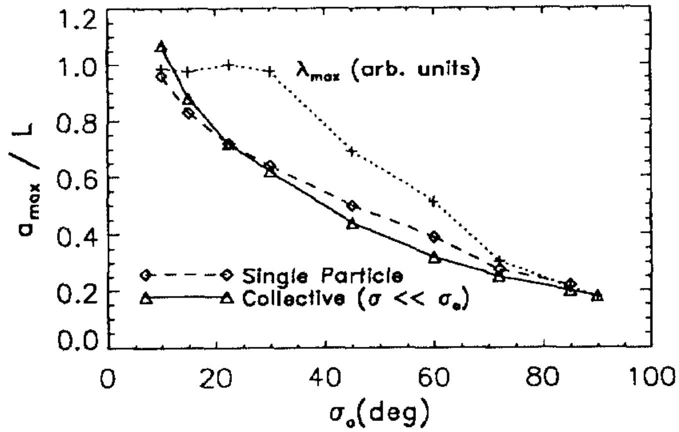

Figure 3: The dynamic aperture of a "one-term" sinusoidal periodic lattice for both space-charge dominated ($\sigma \ll \sigma_o$) and emittance-dominated ($\sigma = \sigma_o$) beams. The dotted curve labeled λ_{max} refers to the maximum line charge density that can be transported ($\sigma \ll \sigma_o$) with negligible particle loss.

envelope *edge* (as opposed, for example, to an algorithm that uses area-weighting). For larger values of a_b/L, this scheme becomes inaccurate and a full particle simulation must be done iteratively to obtain the predicted macroscopic match quantities.

Even when the macroscopic match is "correct", the microscopic deviation of the beam's internal profile from the nonlinear equilibrium value can lead to strong emittance growth. In agreement with expectations from Eq. (6), it appears that the equilibrium profile must have a space-charge density $\rho(r)$ increasing with r and a small, but nonzero octupole moment. Our simulations show both characteristics developing within a few plasma periods when $a_b/L \geq 0.2$. It then takes ≈30 lattice periods for the beam to settle down near its new equilibrium. This adjustment normally leads to the formation of a halo in velocity space.

When $a_b/L \leq 0.1$, the focusing nonlinearities are small and there is very little emittance growth for a well-matched beam. Fig. 2 plots the ratio of final to initial emittance versus beam radius for three values of σ_o. The initial beam brightness was kept constant (*i.e.* $\varepsilon \propto \lambda^{1/2}$) and the tune depression was $\sim 12:1$ for $\sigma_o = 72°$ and $a_b/L \approx 0.08$. We define the maximum dynamic aperture a_{max} as the radius beyond which significant numbers of beam particles will be lost. Plots of a_{max} versus σ_o for both space-charge and emittance-dominated beams are shown in Fig. 3. For $\sigma_o \approx 72°$, the instability boundary appears to be associated with unstable fixed points whose (undepressed) pahse advance is 90°. When σ_o is relatively small, there is not such a clear association with fixed points. We find it intriguing that throughout this large range in σ_o, the instability boundary is barely perturbed by the presence of strong space-charge effects, at least for well-matched beams.

Fig. 3 also plots the (normalized) maximum line charge density that can be transported over 100 lattice periods with little or no loss. We stress that although one can transport greater λ at $\sigma_o = 30°$ than at 72°, the emittance growth is so severe for $\lambda \geq 0.25\lambda_{max}$ at 30° that few applications could use the resultant beam. Scans of emittance growth for well-matched beams with $\lambda = 0.8\lambda_{max}(\sigma_o = 72°)$ versus σ_o show a minimum value in the 65° to 75° range. The growth is larger for either much lower σ_o values or higher values (where particle loss, too, is a problem). Consequently, our present results support the present bias in HIF driver design to set $\sigma_o \approx 72°$.

This paper is dedicated with deep affection to the memory of our co-author, L. J. Laslett.

References

[1] P. Krejcik, "Nonlinear Quadrupole End-Field Effects in the CERN Antiproton Accumulators," *Conference Record of the 1987 IEEE Particle Accelerator Conference*, Vol. 2, pp. 1278-1280.

[2] Laslett, L.J., Caspi, S., Helm, M., *Particle Accel.*, **22**, 1 (1987).

[3] Haber, I., "High Current Simulation Codes," *High Current, High Brightness, High Duty Factor Ion Injectors*, Ed. George H. Gillespie *et al.*, **AIP Conf. Proc. 139**, (AIP, New York, 1986), p. 107.